CrossMark

ONCOLOGY

Diagnostic performance of MR imaging findings and quantitative values in the differentiation of seromucinous borderline tumour from endometriosis-related malignant ovarian tumour

Yasuhisa Kurata[1] · Aki Kido[1] · Yusaku Moribata[1] · Kyoko Kameyama[1] ·
Yuki Himoto[1] · Sachiko Minamiguchi[2] · Ikuo Konishi[3] · Kaori Togashi[1]

Abstract

Objectives To evaluate the diagnostic performance of quantitative values and MRI findings for differentiating seromucinous borderline tumours (SMBTs) from endometriosis-related malignant ovarian tumours (MT).

Methods This retrospective study examined 19 lesions from SMBT and 84 lesions from MT. The following quantitative values were evaluated using receiver-operating characteristic analysis: overall and solid portion sizes, fluid signal intensity (SI), degree of contrast-enhancement, and mean and minimum apparent diffusion coefficient (ADC) values of the solid portion. Two radiologists independently evaluated four MRI findings characteristic of SMBT, fluid SI on the T1-weighted image and SI of the solid portion on diffusion-weighted image. The diagnostic values of these findings and interobserver agreement were assessed.

Results For diagnosing SMBT, the mean ADC value of the solid portion showed the greatest area under the curve (0.860) (cut-off value: 1.31×10^{-3} mm^2/s, sensitivity: 1.00, specificity: 0.61). The T2-weighted image (T2WI) high SI solid portion was the most useful finding, with high specificity and interobserver agreement (sensitivity,

0.58; specificity, 0.95–0.96, kappa = 0.96), followed by T2WI low SI core (sensitivity, 0.48–0.63; specificity, 0.98, kappa = 0.68).

Conclusion Mean ADC values of the solid portion, T2WI high SI solid portion, and T2WI low SI core were useful for differentiating SMBT from MT.

Key Points
- *SMBT is a newly categorised ovarian tumour often associated with endometriosis.*
- *Differentiation of SMBT from endometriosis-related malignant ovarian tumour is clinically important.*
- *Diagnostic performances of quantitative values and MRI findings were evaluated.*
- *Mean ADC value of the solid portion was the most useful value.*
- *"T2WI high SI solid portion" was the most useful MRI finding.*

Keywords Seromucinous borderline tumour · Clear cell carcinoma · Endometrioid carcinoma · Endometriosis · MRI

✉ Aki Kido
akikido@kuhp.kyoto-u.ac.jp

1 Department of Diagnostic Imaging and Nuclear Medicine, Kyoto University Graduate School of Medicine, 54 Kawahara-cho, Shogoin, Sakyoku Kyoto 606-8507, Japan

2 Department of Diagnostic Pathology, Kyoto University Graduate School of Medicine, 54 Kawahara-cho, Shogoin, Sakyoku Kyoto, Japan

3 Department of Gynecology and Obstetrics, Kyoto University Graduate School of Medicine, 54 Kawahara-cho, Shogoin, Sakyoku Kyoto, Japan

Abbreviations and acronyms

MMBT	Müllerian mucinous borderline tumour
MEBT	Müllerian mixed epithelial borderline tumour
SMBT	Seromucinous borderline tumour
CCC	Clear cell carcinoma
EC	Endometrioid carcinoma
DWI	Diffusion-weighted image
ADC	Apparent diffusion coefficient
SI	Signal intensity

Introduction

Seromucinous borderline tumour (SMBT) is a newly categorised tumour in the 2014 revised WHO classification of tumours of the female reproductive organs [1]. Tumours previously diagnosed as endocervical-like mucinous borderline tumour/Müllerian mucinous borderline tumour (MMBT) and Müllerian mixed epithelial borderline tumour (MEBT) are now categorised as SMBTs. Like other subtypes of ovarian borderline tumour, SMBT is probably a precursor lesion of a malignant tumour, though seromucinous carcinoma is very rare [2]. Reportedly, about 30–70 % of SMBTs are associated with endometriosis [3, 4]. Along with clear cell carcinoma (CCC) and endometrioid carcinoma (EC), which are malignant tumours often arising from endometriotic cysts, SMBT is thought to be an endometriosis-related ovarian neoplasm. On average, about 8–59 % of CCCs and 9–42 % of ECs were reported to be associated with endometriosis [5]. These endometriosis-related ovarian neoplasms are now attracting attention because they show common molecular genetic changes such as inactivating mutation of the ARID1A tumour suppressor gene [6, 7]. Although precise differentiation of SMBT from CCC and EC is often difficult preoperatively, these tumours show entirely different clinical features. More than 80 % of SMBTs are described as stage I, for which even advanced stage or recurrent SMBT patients had a good prognosis [8, 9]. In addition, SMBT is described as occurring in young women (average 36–49 years old) [8, 9]. Therefore, conservative surgery can be regarded as an option for pre-menopausal women, especially those of reproductive age who desire to preserve fertility [10–12]. However, CCC and EC are associated with a poorer prognosis [13, 14]. Consequently, in principle, staging laparotomy is recommended for patients with CCC and EC, even at an early stage. Regarding surgical management, lymphadenectomy is not indicated for patients with borderline tumours because the recurrence and survival rates for patients with positive or negative lymph nodes are similar. In contrast, systemic pelvic and para-aortic lymph node dissection is generally recommended for patients with ovarian cancer [11]. For these reasons, the preoperative differentiation of SMBT from CCC and EC is clinically very important. Although potentially useful MR imaging findings with radiologic-pathologic correlation for diagnosing SMBT have been reported, their actual diagnostic values have not been evaluated [15, 16]. No report of the literature describes a study conducted to assess the differentiation of endometriosis-related ovarian neoplasms.

The objective of this study was to present MRI findings and quantitative values that are expected to be useful for differentiating SMBT from malignant tumours arising from endometriotic cysts and to determine their diagnostic value.

Materials and methods

Our institutional review board approved this single-centre retrospective study. The requirement for written informed consent was waived.

Patients

Pathological and radiological records collected at our institute between January 2000 and October 2015 were searched for ovarian SMBT, CCC, and EC. Results revealed 25 SMBT patients, among whom 6 patients had bilateral lesions. Patients without preoperative MRI ($n = 2$), those without pathological evidence of endometriosis ($n = 4$), those with lesions too small overall to detect on MRI (2 lesions), and those without detailed clinical records ($n = 3$) were excluded from the study. Also, 88 CCC patients were identified. Those without preoperative MRI ($n = 15$), those without pathological evidence of endometriosis ($n = 16$), those without detailed clinical records ($n = 3$), and those presenting recurrent lesions ($n = 4$) were all excluded. One patient with coexistent lesions of SMBT and CCC was also excluded. In addition, 52 EC patients were identified, among whom four patients presented bilateral lesions. Patients without preoperative MRI ($n = 5$), those without pathological evidence of endometriosis ($n = 12$), and those presenting poor image quality ($n = 1$) were excluded. Three patients with coexistent lesion of SMBT and EC were also excluded. This study examined 16 SMBT patients (19 lesions), 49 CCC patients (49 lesions), and 31 EC patients (35 lesions). When statistical analysis on MR imaging findings and quantitative values was performed, CCC and EC were both classified as malignant tumour.

MRI protocol

For this study, MRI was performed using a 1.5-T unit (Symphony or Avanto, Siemens Health Care, Erlangen, Germany; Signa, General Electric Medical Systems, Milwaukee, WI, USA) or a 3.0-T unit (Trio, Skyra; Siemens Health Care, Erlangen, Germany) using a phased-array coil. Before MR examination, 20 mg of butyl scopolamine (Buscopan; Nippon Boehringer Ingelheim, Tokyo, Japan) was administered intramuscularly before acquisition. Our routine MR images were sagittal T1-wighted image (T1WI), T2-weighted image (T2WI), and diffusion-weighted image (DWI), axial T1WI with fat suppression and T2WI, and sagittal and

axial contrast-enhanced T1WI with or without fat suppression. Contrast-enhanced T1WI was obtained upon administration of the gadolinium contrast agent (Magnevist; Bayer Yakuhin, Ltd., Osaka, Japan) at a dose of 0.2 mmol/kg intravenously. The imaging parameters are presented in Table 1. Selected b values of each patient had some variation: $b = 1000$ s/mm^2, $b = 0$ and 1000 s/mm^2, $b = 0$, 500, and 1000 s/mm^2, and $b = 0$, 100, 500, 1000 s/mm^2. When at least two b values were referred, apparent diffusion coefficient (ADC) values were calculated. Contrast-enhanced MR images were obtained in 14 of 16 SMBT patients (17 of 19 lesions), 47 of 49 CCC patients (47 of 49 lesions), and 31 of 31 EC patients (35 of 35 lesions). DWI was obtained in 13 of 16 SMBT patients (15 of 19 lesions), 43 of 49 CCC patients (43 of 49 lesions), and 28 of 31 EC patients (31 of 35 lesions). The ADC map was referenced for 12 of 16 SMBT patients (15 of 19 lesions), 40 of 49 CCC patients (40 of 49 lesions), and 24 of 31 EC patients (26 of 35 lesions).

Clinical characteristics

One board-certified radiologist (Y.K.) with 9 years of experience in gynaecological radiology searched the clinical records for patients' clinical information including pathology reports. We investigated the number (percentage) of patients who exhibited increased concentrations of CEA (≥5.0 ng/ml), CA19-9 (≥37.0 U/ml), and CA125 (≥35.0 U/ml). Bilaterality of the tumour and the presence of endometrial lesions were also examined in the pathology report.

Quantitative analysis

The same radiologist (Y.K.) performed the quantitative evaluation of each tumour and determined the following parameters: overall and solid portion sizes of the tumour, signal intensity (SI) on T1WI of the iliopsoas muscle, and fluid in the cystic portion of the tumour when the tumour comprised both solid and cystic portions, SI of the solid portion on pre- and post-contrast-enhanced T1WI, and mean and minimum ADC values of the solid portion. The overall size was defined as the maximal diameter of the tumour, whereas the solid portion size was defined as the height of the solid portion, starting from the tumour wall. All image analyses were performed using the clinical workstation (Centricity RA1000; GE Healthcare, Barrington, IL).

For the measurement of SI and ADC values, polygonal regions of interest (ROIs) were placed on the entire solid portion manually to cover as large an area as possible while avoiding areas such as intratumoral cysts, haemorrhages, and necroses, referring to other sequences such as T2WI and contrast and non-contrast enhanced T1WI. When a given tumour presented multiple solid nodules, the largest nodule was examined. The SI ratio was calculated as follows: fluid SI ratio = fluid SI in the cystic portion of the tumour/SI of the iliopsoas muscle; contrast-enhancement SI ratio = SI of the solid portion on post-contrast enhanced T1WI/SI of the solid portion on pre-contrast enhanced T1WI.

Qualitative analysis

Two board-certified radiologists with 9 years (Y.M.) and 7 years (K.K.) of experience in gynaecological radiology

Table 1 MR imaging parameters

MR parameters	T1WI	T2WI	DWI	CE-T1WI (FSE)	CE-T1WI (GE)
TR (ms)	400-655	3730-7760	2300-5900	450-650	3.2-3.4
TE (ms)	11-30	81-120	63-87	9.3-30	1.2-1.3
FA	80	150	90	90-170	10
Band width (Hz/pixel)	100-140	140-370	1445-2170	125-230	580
Matrix size	527 × 224-348	448-512 × 204-512	128 × 73-128	320-512 × 176-348	320-384 × 198-230
Slice thickness (mm)	4-6	4-5	4-5	4-6	4

TR: repetition time

TE: echo time

FA: flip angle

T1WI: T1-weighted image

T2WI: T2-weighted image

DWI: diffusion-weighted image

CE-T1WI: contrast-enhanced T1-weighted image

FSE: fast spin echo

GE: gradient echo

independently reviewed all images. They were blind to the pathological diagnosis of each tumour. The following four imaging findings were assessed in terms of their presence (positive) or absence (negative): (1) nodule in cyst appearance, (2) papillary solid nodule, (3) T2WI high SI solid portion, and (4) T2WI low SI core. "Nodule in cyst appearance" was defined as positive in cases where the tumour was composed of a cyst and mural nodule. When both readers positively scored a tumour as "nodule in cyst appearance", the fluid SI ratio described above and fluid SI on T1WI described later were evaluated. "Papillary solid nodule" was scored as present when the tumour showed a minute papillary contour on the surface. "T2WI high SI solid portion" was scored positive when the tumour presented a high SI solid portion equal to water or subcutaneous fat. "T2WI low SI core" was scored positive when the intratumoral low intensity solid portion was equal to that of the skeletal muscle on T2WI. Both readers made an effort not to consider intratumoral haemorrhage as a

"T2WI low SI core" by referring to other images such as T1WI with or without contrast medium. Representative MR images accompanying the imaging findings above and the corresponding pathological findings are presented in Fig. 1. The sensitivity, specificity, positive likelihood ratio, and negative likelihood ratio of each image finding were calculated for both readers. The two readers classified fluid SI on T1WI as bright (similar to subcutaneous fat), intermediate (intermediate SI between bright and low), or low (similar to water). The two readers also classified the SI of the solid portion of the tumour on DWI as high (similar to nerve root), moderate (similar to small intestine), or low (similar to background signal). Sensitivity and specificity were calculated with SI on DWI using two criteria: (1) tumours of low SI on DWI were diagnosed as SMBT and (2) tumours of low and moderate SI were diagnosed as SMBT. Representative MR images of SMBT and malignant tumour on DWI and ADC maps are presented in Fig. 2.

Fig. 1 Representative MR appearance of seromucinous borderline tumour (SMBT) and its pathological findings. Axial T2-weighted image (**a**) shows an ovarian tumour composed of cyst and mural nodule. The papillary-shaped nodule consists of a peripheral high signal intensity portion (*arrow*) and central low signal intensity portion (*arrowhead*). Axial fat suppressed T1-weighted image (**b**) shows high signal intensity fluid in the cyst. Axial contrast-enhancement fat suppressed T1-weighted image (**c**) shows moderate papillary nodule enhancement. The photograph of the surgical specimen of the tumour (**d**) presents the minute papillary architecture of the solid portion. Histological section of the papillary nodule (**e**) shows edematous stroma (*arrowhead*) with a fibrous core (*arrow*) respectively corresponding to the high and low signal intensity portions of T2-weighted images
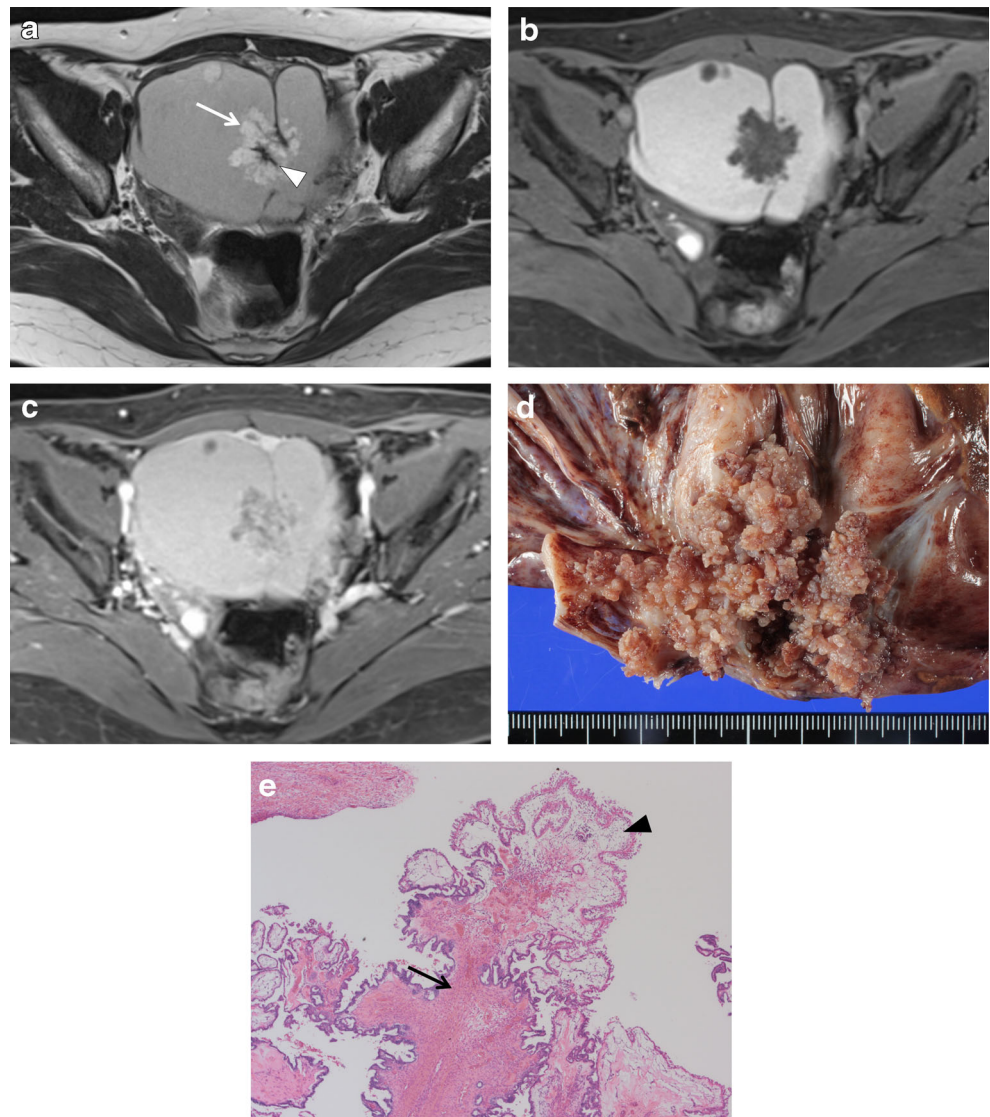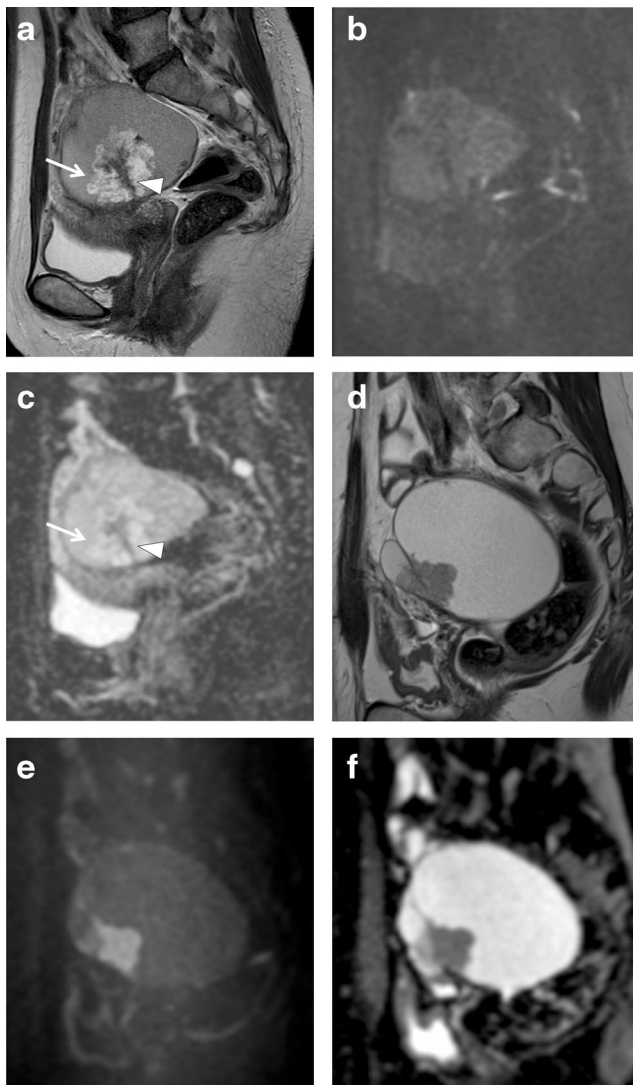
Fig. 2 Representative MR images of seromucinous borderline tumour (SMBT) (**a**–**c**) and endometriosis-related malignant ovarian tumour (**d**–**f**) on diffusion-weighted image (DWI) and apparent diffusion coefficient (ADC) map. (**a**,**d**) Sagittal T2-weighted image shows a tumour composed of cyst and mural nodule. The SMBT nodule consists of a peripheral high signal intensity portion (**a**, *arrow*) and a central low]signal intensity portion (**a**, *arrowhead*). On sagittal DWI (**b**,**e**), the nodule of SMBT shows low signal intensity. That of a malignant tumour shows high signal intensity. On the sagittal ADC map (**c**,**f**), the peripheral portion of the nodule (**c**, *arrow*) of SMBT shows a high ADC value, while the central portion of the nodule (**c**, *arrowhead*) shows a low ADC value compared to the peripheral portion. The nodule of a malignant tumour shows a low ADC value

Statistical analysis

Statistical analyses were performed using a commercially available software package (Medcalc ver. 12.3.0; MedCalc Software, Ostend, Belgium) and EZR (Saitama Medical Center, Jichi Medical University, Saitama, Japan), a graphical user interface for R (The R Foundation for Statistical Computing, Vienna, Austria) [17]. One-way analysis of

variance with the *post hoc* Bonferroni test was applied to compare the age between groups. The frequency of patients with elevated tumour markers, occurrence of bilateral ovarian tumours and coexistent uterine endometrial cancers, each imaging finding, fluid SI on T1WI, and SI of the solid portion on DWI were analysed using Fisher's two-sided exact test. Mann-Whitney U tests were applied to compare non-normally distributed continuous variables between the SMBT and malignant tumour groups. Receiver-operating characteristic (ROC) curves were calculated for MR quantitative values. The ROC curve was used to calculate the area under the curve (AUC) and to ascertain the optimal cut-off value for diagnosing SMBT, defined as the value providing the largest sum of sensitivity and specificity. The degree of interobserver agreement was calculated using kappa statistics in the evaluation of imaging findings and the weighted kappa statistics for the assessment of fluid SI on T1WI and SI of the solid portion on DWI. A kappa value of 0.21–0.40 was inferred as fair agreement, 0.41–0.60 moderate agreement, 0.61–0.80 substantial agreement, and 0.81–1.00 excellent agreement [18]. All *p*-values < 0.05 were considered statistically significant.

Results

Clinical characteristics

Age, frequency of patients with elevated tumour markers, bilateral tumour occurrence, and coexistence of uterine endometrial carcinoma in each pathological group are presented in Table 2. EC patients were significantly younger than the CCC patients were ($p = 0.007$). No other significant difference was found between the other groups. When comparison between SMBT and malignant tumour was performed, no significant difference was found in age ($p = 0.69$). Regarding tumour markers, no significant difference was found between the groups. Bilateral ovarian tumours occurred in SMBT and EC, respectively, at frequencies of 19 % and 13 %. No significant difference was found when comparing SMBT vs. EC or SMBT vs. malignant tumour ($p = 1.00$ and $p = 0.088$, respectively). Coexistent uterine endometrial carcinoma was found only in the EC patients (42 %). Significant difference was found between EC and the other types of tumours ($p < 0.001$).

Quantitative evaluation

The results of the quantitative evaluation of SMBT and malignant tumours are presented in Table 3. The overall and solid portion sizes of SMBT were both significantly smaller than those of malignant tumour ($p = 0.014$ and $p = 0.003$, respectively). The fluid SI ratio was calculated for 19/19 lesions of SMBT and for 73/84 lesions of malignant tumour. The fluid SI

Table 2 Clinical features of each pathological group

	SMBT ($n = 16$)	CCC ($n = 49$)	EC ($n = 31$)	p value
Age	48.6 ± 12.4 (24-66)	52.6 ± 10.5 (32-75)	45.3 ± 7.6 (34-58)	0.008
CA19-9 elevation	10 (63 %)	23 (47 %)	11 (35 %)	0.23
CA125 elevation	10 (63 %)	26 (60 %)	23 (74 %)	0.15
CEA elevation	0 (0 %)	3 (6 %)	4 (13 %)	0.27
Bilateral lesion	3 (19 %)	0 (0 %)	4 (13 %)	0.005
Endometrial carcinoma	0 (0 %)	0 (0 %)	13 (42 %)	<0.001

Data are presented as mean ± standard deviation (min-max) for age, and n (%) for patients with elevated tumour markers, bilateral lesions, and coexistent uterine endometrial carcinoma

SMBT: seromucinous borderline tumour

CCC: clear cell carcinoma

EC: endometrioid carcinoma

ratio of SMBT was significantly higher than that of a malignant tumour ($p = 0.031$). No significant difference was found in the contrast-enhancement ratio between the two groups ($p = 0.076$). Mean and minimum ADC values of the solid portion of SMBT were both higher than those of malignant tumours ($p < 0.001$ and $p = 0.026$, respectively). The minimum size of the ROI on the solid portion was 25 mm^2 for SMBT and 83 mm^2 for a malignant tumour.

ROC analysis

The mean ADC value achieved the highest AUC (0.860), followed by solid portion size (AUC = 0.718), minimum ADC value (AUC = 0.685), overall size (AUC = 0.681), fluid SI ratio (AUC = 0.660), and contrast-enhancement ratio (AUC = 0.638) (Fig. 3). The cut-off value, sensitivity, and specificity of each parameter were the following: mean ADC value [10^{-3} mm^2/s] (1.31, 1.00, 0.61), solid portion size [cm] (2.10, 0.74, 0.66), minimum ADC value [10^{-3} mm^2/s] (1.03, 0.67, 0.86), overall size [cm] (6.80, 0.63, 0.75), fluid SI ratio

(2.07, 0.68, 0.65), and contrast-enhancement ratio (1.84, 0.77, 0.57).

Qualitative evaluation

Results of the evaluation of MR imaging findings are presented in Table 4. No significant difference was found for "nodule in cyst appearance". "Papillary solid nodule", "T2WI high SI solid portion", and "T2WI low SI core" were frequently found in SMBT at a significant level ($p < 0.001$, all findings for both readers). Interobserver agreement was excellent in relation to "nodule in cyst appearance" and "T2WI high SI solid portion" (kappa = 0.81 and 0.96, respectively), moderate in relation to "papillary solid nodule" (kappa = 0.54), and substantial in relation to "T2WI low SI core" (kappa = 0.68). Table 5 presents the respective sensitivity, specificity, positive likelihood ratio, and negative likelihood ratio of these findings. Fluid SI of SMBT on T1WI was the following: low, 4 (21 %) and 4 (21 %); intermediate, 6 (32 %) and 4 (21 %); high, 9 (47 %) and 11 (58 %), respectively, for readers 1 and 2. Those of the malignant tumour were the following: low, 25 (34 %) and 24

Table 3 Results of MR quantitative evaluation

	SMBT ($n = 19$)	Malignant tumour ($n = 84$)	p value
Overall size (cm)	6.7 (5.1-9.55)	10.05 (6.9-14.0)	0.014
Solid portion size (cm)	1.8 (0.9-2.5)	3.45 (1.9-5.63)	0.003
Fluid SI ratio	2.88 (1.71-3.41)	1.59 (1.14-2.71)	0.031
Contrast-enhancement ratio	1.72 (1.59-1.84)	1.98 (1.66-2.23)	0.076
Mean ADC value (10^{-3} mm^2/s)	1.77 (1.48-1.88)	1.20 (1.04-1.40)	<0.001
Minimum ADC value (10^{-3} mm^2/s)	1.20 (0.73-1.33)	0.81 (0.65-0.925)	0.026

Data are presented as median (interquartile range)

The fluid SI ratio was calculated in 19/19 of SMBTs and 73/84 of malignant tumours, contrast-enhancement ratio 17/19 of SMBTs and 78/84 of malignant tumours, mean and minimum ADC value 15/19 of SMBT and 66/84 of malignant tumour.

SMBT: seromucinous borderline tumour

SI: signal intensity

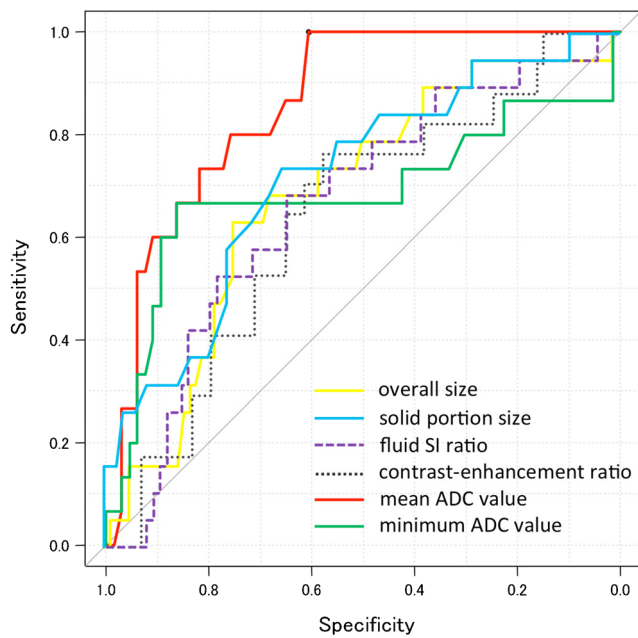ADC: apparent diffusion coefficient

Fig. 3 Receiver operating characteristic (ROC) curves of the quantitative values

(33 %); intermediate, 23 (32 %) and 27 (37 %); bright, 25 (34 %) and 22 (30 %), respectively, for the readers. No significant difference was found between the two groups ($p = 0.50$ and 0.10 for readers 1 and 2, respectively). Interobserver agreement was substantial (kappa = 0.76). SI of the solid portion of SMBT on DWI was the following: low, 4 (27 %) and 7 (47 %); moderate, 6 (40 %) and 4 (27 %); high, 5 (33 %) and 4 (27 %) for readers 1 and 2. Those of malignant tumour were the following: low, 1 (1.3 %); moderate, 7 (9.3 %); high 66 (88 %) for both readers. A significant difference was found for SI on DWI between the two groups ($p < 0.001$ for both readers). When tumours of low SI on DWI were diagnosed as SMBT, sensitivity and specificity with 95 % confidence interval were 0.27 (0.078–0.55) and 0.99 (0.93–1.00) for reader 1 and 0.47 (0.21–0.73) and 0.99 (0.93–1.00) for reader 2. When tumours of low and moderate SI were diagnosed as

SMBT, the sensitivity and specificity were 0.67 (0.38–0.88) and 0.89 (0.80–0.95) respectively for reader 1 and 0.73 (0.45–0.92) and 0.89 (0.80–0.95) respectively for reader 2. Interobserver agreement was substantial (kappa = 0.78).

Discussion

Our study assessed the diagnostic value of a set of quantitative values and MR imaging findings for the differentiation of SMBT from endometriosis-related malignant ovarian tumour. Among the quantitative values, the mean ADC value of the solid portion was the most useful quantitative value with high sensitivity for diagnosing SMBT. In relation to MR imaging findings, "T2WI high SI solid portion" and "T2WI low SI core" showed high specificity for the diagnosis of SMBT. The T2WI high SI solid portion particularly showed excellent interobserver agreement.

Our results demonstrated that the mean ADC value of the solid portion was the most useful quantitative value. Indeed, the mean ADC value of SMBT was significantly higher than that of a malignant ovarian tumour. It achieved the highest AUC, high sensitivity, and moderate specificity. Although the minimum ADC value also showed significant difference between the two groups, it showed lower diagnostic performance than the mean ADC value. DWI can create image contrast depending on the difference of tissue molecular diffusion; it also permits quantitative evaluation using ADC values [19, 20]. A reduced ADC value is related to the increased cellular density of tumours. Several reports in the literature have described that DWI and ADC values were useful for the differentiation of benign from malignant ovarian tumours [21–25]. Our results showed good agreement with those of earlier studies. The mean ADC value of the solid portion achieved high diagnostic performance attributable to the high cellularity of malignant tumour and also to the edematous stromal nature of SMBT, which contributes to the high ADC value. The lower diagnostic performance of the

Table 4 Results of the evaluation of MR imaging findings and interobserver agreement

MR imaging finding	SMBT ($n = 19$)		Malignant tumour ($n = 84$)		p value		Kappa value
	Reader 1	Reader 2	Reader 1	Reader 2	Reader 1	Reader 2	
Nodule in cyst appearance	19 (100 %)	19 (100 %)	76 (90 %)	75 (89 %)	0.35	0.2	0.81 [0.60-1.00]
Papillary solid nodule	11 (58 %)	13 (68 %)	6 (7.1 %)	17 (20 %)	<0.001	<0.001	0.54 [0.36-0.73]
T2WI high SI solid portion	11 (58 %)	11 (58 %)	3 (3.6 %)	4 (4.8 %)	<0.001	<0.001	0.96 [0.89-1.00]
T2WI low SI core	9 (47 %)	12 (63 %)	2 (2.4 %)	2 (2.4 %)	<0.001	<0.001	0.68 [0.46-0.90]

Data are n (%) for each imaging finding

Kappa value and 95 % confidence interval are shown

T2WI: T2-weighted image

SI: signal intensity

Table 5 Summary of the sensitivity, specificity, positive likelihood ratio (PRL), and negative likelihood ratio (NRL) associated with the MR imaging findings

MR imaging finding	Reader 1				Reader 2			
	Sen	Spe	PRL	NRL	Sen	Spe	PRL	NRL
Nodule in cyst appearance	100 % (75-100)	9 % (4-18)	1.11 (1.03-1.19)	0	100 % (75-100)	11 % (5-19)	1.12 (1.04-1.21)	0
Papillary solid nodule	58 % (34-80)	93 % (85-97)	8.11 (3.43-19.18)	0.45 (0.27-0.77)	68 % (43-87)	80 % (70-88)	3.38 (2.00-5.70)	0.40 (0.20-0.77)
T2WI high SI solid portion	58 % (34-80)	96 % (90-99)	16.21 (5.00-52.52)	0.44 (0.26-0.74)	58 % (34-80)	95 % (88-99)	12.16 (4.34-34.07)	0.44 (0.26-0.75)
T2WI low SI core	48 % (24-71)	98 % (92-100)	19.90 (4.67-84.73)	0.54 (0.35-0.83)	63 % (38-84)	98 % (92-100)	26.53 (6.47-108.8)	0.38 (0.21-0.68)

Data are % (95 % confidence interval) for sensitivity and specificity, and values (95 % confidence interval) for PRL and NRL

Sen: sensitivity

Spe: specificity

T2WI: T2-weighted image

SI: signal intensity

minimum ADC value is expected to be the result of a "T2-blackout effect" caused by the fibrous core of SMBT: a fibrous core exhibits low SI on a DWI with a low b value. It therefore has less SI to lose on images with higher b values, resulting in low ADC values [26]. Even when SMBT had a fibrous core, it usually occupied only a small area of the tumour. For that reason, it would probably have only a negligible effect on the mean ADC value. The solid portion size parameter revealed moderate diagnostic performance. Tanaka et al. reported that the sizes of both the overall cyst and mural nodules of an endometriotic cyst with malignant conditions were significantly larger than those of an endometriotic cyst with benign conditions [27]. In their research, a borderline tumour was categorised as an endometriotic cyst with malignant condition. They did not compare borderline and malignant tumours.

Our study also revealed several MR imaging findings with high specificity for the diagnosis of SMBT: "papillary solid nodule", "T2WI high SI solid portion", and "T2WI low SI core". These findings correspond to the gross papillary architecture, edematous stroma, and fibrous core of solid nodules, which are all pathological findings characteristic of SMBT [9, 13]. "T2WI high SI solid portion" showed high specificity and excellent interobserver agreement. This was a simple finding, which, when present, was easily recognisable by both readers. Although the sensitivity might not be sufficient for the detection of all cases of SMBT, high specificity is expected to contribute to the consideration for conservative surgery. The "T2WI low SI core" showed high sensitivity and substantial interobserver agreement. The fibrous core was a minute structure even when present. It was sometimes difficult to recognise in cases of a small solid portion. This might explain the lower interobserver agreement than that of a "T2WI high SI solid portion". "Papillary solid nodule" showed lower

interobserver agreement than those of other findings, probably because recognition of the papillary architecture was difficult, especially in the case of small tumours as a result of the partial volume effect.

As for SI on DWI, low SI on DWI is expected to be highly suggestive of SMBT, whereas moderate SI would indicate the possibility of SMBT. Some SMBTs exhibited high intensity on DWI, probably because of the "T2 shine-through effect", i.e., edematous stroma of SMBT presenting high SI on T2WI could have contributed to the high SI on DWI [28].

Our study has several limitations. First, this research was a retrospective study in which the SMBT patient sample size was small. A larger prospective study would be preferred, but such a study might be practically difficult to achieve because of the rare occurrence of SMBT. Second, the MRI machines and their respective acquired sequence parameters had some variation because we included patients for a long period of time. In addition to MR field strength (1.5 T or 3.0 T), the variation of b-values used in our study to calculate ADC values (b = 0 and 1000 s/mm^2, b = 0, 500, and 1000 s/mm^2 and b = 0, 100, 500, 1000 s/mm^2) might affect the ADC values. Another limitation of the ADC value was that the smaller ROI of the solid portion of SMBT compared to malignant tumour (minimum ROI for SMBT; 25 mm^2 vs. malignant tumour; 83 mm^2) might contribute to the higher ADC value of the solid portion of SMBT because of the partial volume effect. As for the contrast enhancement of the tumours, we only analysed the contrast enhancement ratio, but not dynamic contrast enhanced (DCE) images. Thomassin-Naggara et al. demonstrated the utility of DCE MRI for distinguishing among benign, borderline, and malignant epithelial ovarian tumours [29]. Analysing the time intensity curve of the solid portion is expected to be useful for differentiating SMBT from endometriosis-related malignant

ovarian tumour. In addition, in some cases, DWI or contrast-enhanced images were not available. This was unavoidable, however, because long-term patients were included in the study because of the rare prevalence of SMBT. Finally, only patients who underwent MRI were enrolled, which might have led to a selection bias.

In conclusion, this study demonstrated clinically useful quantitative values and MR imaging findings for the differentiation of SMBT from endometriosis-related malignant ovarian tumour. Regarding quantitative values, the mean ADC value of the solid portion of the tumour showed the best diagnostic performance and was associated with high sensitivity. Regarding imaging findings, "T2WI high SI solid portion" and "T2 low SI core" were regarded as useful findings with high specificity. Low SI of the solid portion of the tumour on DWI was also a useful finding, suggestive of SMBT. Combining quantitative values of high sensitivity with the MR imaging findings of high specificity for diagnosing SMBT is expected to be valuable in clinical practice.

References

1. Kurman RJ, Carcangiu ML, Herrington CS, Young RH (2014) WHO classification of tumours of female reproductive organs. International Agency for Research on Cancer, Lyon
2. Taylor J, McCluggage WG (2015) Ovarian seromucinous carcinoma: report of a series of a newly categorized and uncommon neoplasm. Am J Surg Pathol 39:983–992
3. Rutgers JL, Scully RE (1988) Ovarian Mullerian mucinous papillary cystadenomas of borderline malignancy. A clinicopathologic analysis. Cancer 61:340–348
4. Kim KR, Choi J, Hwang JE et al (2010) Endocervical-like (Müllerian) mucinous borderline tumours of the ovary are frequently associated with the KRAS mutation. Histopathology 57:587–596
5. Yoshikawa H, Jimbo H, Okada S et al (2000) Prevalence of endometriosis in ovarian cancer. Gynecol Obstet Invest 50:11–17
6. Maeda D, Shih I-M (2013) Pathogenesis and the role of ARID1A mutation in endometriosis-related ovarian neoplasms. Adv Anat Pathol 20:45–52
7. Wu CH, Mao T-L, Vang R et al (2012) Endocervical-type mucinous borderline tumors are related to endometrioid tumors based on mutation and loss of expression of ARID1A. Int J Gynecol Pathol 31: 297–303
8. Shappell HW, Riopel MA, Smith Sehdev AE et al (2002) Diagnostic criteria and behavior of ovarian seromucinous (endocervical-type mucinous and mixed cell-type) tumors: atypical proliferative (borderline) tumors, intraepithelial, microinvasive, and invasive carcinomas. Am J Surg Pathol 26:1529–1541
9. Rodriguez IM, Irving JA, Prat J (2004) Endocervical-like mucinous borderline tumors of the ovary: a clinicopathologic analysis of 31 cases. Am J Surg Pathol 28:1311–1318
10. Coumbos A, Sehouli J, Chekerov R et al (2009) Clinical management of borderline tumours of the ovary: results of a multicentre survey of 323 clinics in Germany. Br J Cancer 100:1731–1738
11. Fischerova D, Zikan M, Dundr P, Cibula D (2012) Diagnosis, treatment, and follow-up of borderline ovarian tumors. Oncologist 17: 1515–1533
12. Lalwani N, Shanbhogue AKP, Vikram R et al (2010) Current update on borderline ovarian neoplasms. Am J Roentgenol 194:330–336
13. Seidman JD, Cho KR, Ronnett BM, Kurman RJ (2011) Surface epithelial tumors of the ovary. In: Blaustein's Pathol. Female Genit. Tract. Springer US, Boston, MA, pp 679–784
14. Sugiyama T, Kamura T, Kigawa J et al (2000) Clinical characteristics of clear cell carcinoma of the ovary: A distinct histologic type with poor prognosis and resistance to platinum-based chemotherapy. Cancer 88:2584–2589
15. Matsubayashi RN, Matsuo Y, Nakazono T et al (2015) Magnetic resonance imaging manifestations of ovarian Mullerian mixed epithelial borderline tumors: imaging and histologic features in comparison with Mullerian mucinous borderline tumors. J Comput Assist Tomogr 39:276–280
16. Kataoka M, Togashi K, Koyama T et al (2002) MR imaging of müllerian mucinous borderline tumors arising from endometriotic cysts. J Comput Assist Tomogr 26:532–537
17. Kanda Y (2013) Investigation of the freely available easy-to-use software "EZR" for medical statistics. Bone Marrow Transplant 48:452–458
18. Landis JR, Koch GG (1977) The measurement of observer agreement for categorical data. Biometrics 33:159–174
19. Namimoto T, Awai K, Nakaura T et al (2009) Role of diffusion-weighted imaging in the diagnosis of gynecological diseases. Eur Radiol 19:745–760
20. Punwani S (2011) Diffusion weighted imaging of female pelvic cancers: concepts and clinical applications. Eur J Radiol 78:21–29
21. Zhao SH, Qiang JW, Zhang GF et al (2014) Diffusion-weighted MR imaging for differentiating borderline from malignant epithelial tumours of the ovary: pathological correlation. Eur Radiol 24: 2292–2299
22. Fujii S, Kakite S, Nishihara K et al (2008) Diagnostic accuracy of diffusion-weighted imaging in differentiating benign from malignant ovarian lesions. J Magn Reson Imaging 28:1149–1156
23. Thomassin-Naggara I, Daraï E, Cuenod CA et al (2009) Contribution of diffusion-weighted MR imaging for predicting benignity of complex adnexal masses. Eur Radiol 19:1544–1552
24. Takeuchi M, Matsuzaki K, Nishitani H (2010) Diffusion-weighted magnetic resonance imaging of ovarian tumors: differentiation of benign and malignant solid components of ovarian masses. J Comput Assist Tomogr 34:173–176
25. Li W, Chu C, Cui Y et al (2012) Diffusion-Weighted MRI: a useful technique to discriminate benign versus malignant ovarian surface epithelial tumors with solid and cystic components. Abdom Imaging 37:897–903
26. Siegelman ES, Oliver ER (2012) MR Imaging of endometriosis: ten imaging pearls. Radiographics 32:1675–1691
27. Tanaka YO, Okada S, Yagi T et al (2010) MRI of endometriotic cysts in association with ovarian carcinoma. Am J Roentgenol 194: 355–361
28. Burdette JH, Elster AD, Ricci PE (1999) Acute cerebral infarction: quantification of spin-density and T2 shine-through phenomena on diffusion-weighted MR images. Radiology 212:333–339
29. Thomassin-Naggara I, Daraï E, Cuenod CA et al (2008) Dynamic contrast-enhanced magnetic resonance imaging: a useful tool for characterizing ovarian epithelial tumors. J Magn Reson Imaging 28:111–120